Supporting Information

Madasu et al. 10.1073/pnas.1307235110

Fig. S1. Alignment of surface cell antigen 2 (Sca2) sequences from different *Rickettsia* species. Uniprot accession codes are: *Rickettsia conorii*, Q92JF7; *Rickettsia parkeri*, D7RFH5; *Rickettsia rickettsii*, Q3L8P4; *Rickettsia africae* Q3L8Q6; *Rickettsia peacockii*, C4K198; *Rickettsia canadensis*, A8EXE8. A bar on top of the sequences highlights the various domains of Sca2 (colored according to Fig. 1*A*).

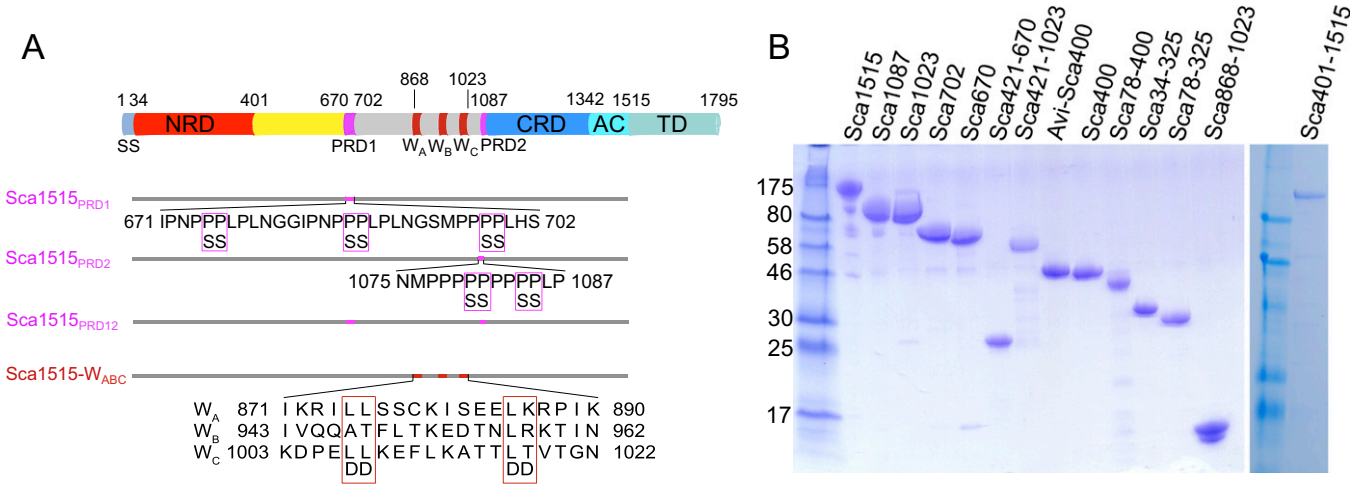

Fig. S2. Mutants and constructs of Sca2. (*A*) Design of Sca1515 constructs containing mutations in the proline-rich domains (PRDs) and WH2 domains. The specific mutations are highlighted in boxes, colored according to the domain diagram. (*B*) SDS/PAGE of some of the Sca2 constructs expressed for this study, after removal of purification tags and additional purification through a Superdex-200 gel-filtration column. Note that some of the constructs were prone to degradation, particularly Sca1515. To alleviate this problem, proteins were used in biochemical assays immediately after purification. Additionally, residues R400 and K420 in a predicted disordered loop were identified by mass spectrometry as the primary sites of degradation. Mutations R400G and K420Q were introduced into constructs extending C-terminally to residue 400, which substantially reduced degradation and had no noticeable effect on activity.

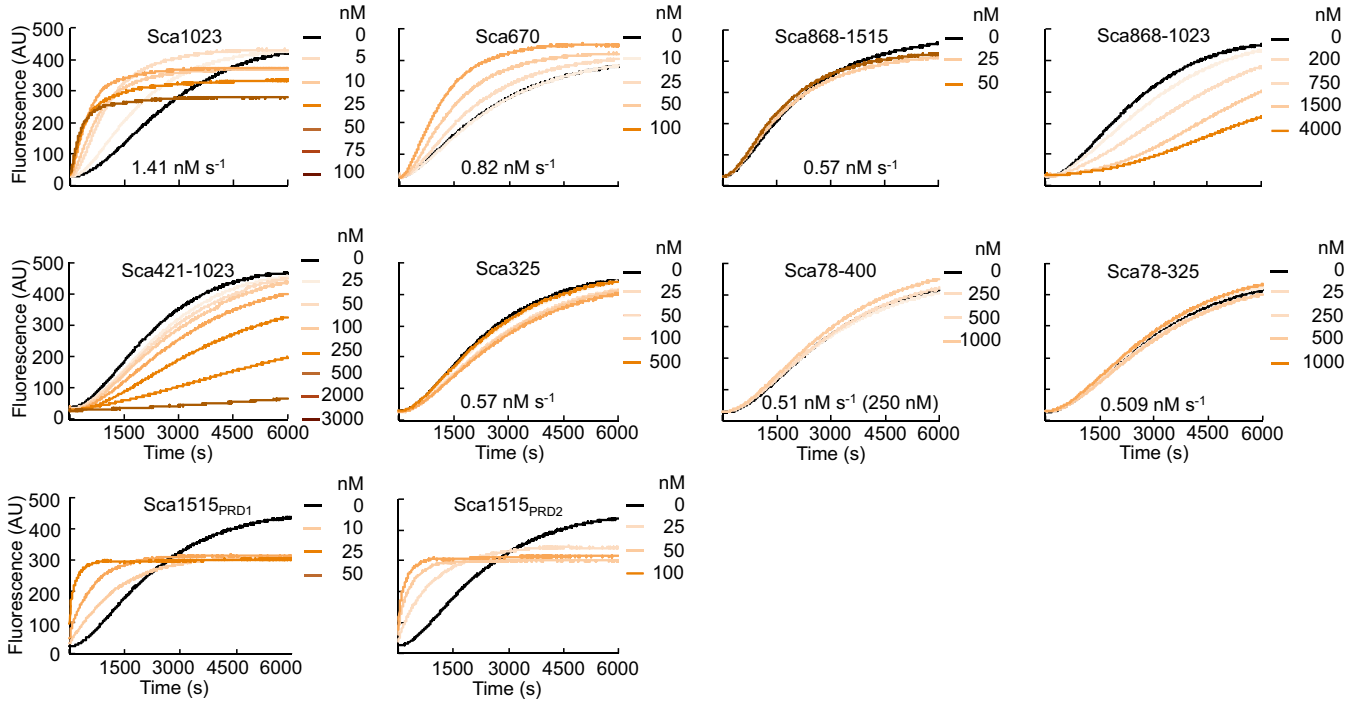

Fig. S3. Time course of polymerization of 2 μM Mg-ATP-actin (6% pyrene-labeled) alone (black) or with increasing concentrations of Sca2 constructs, as indicated. Also shown are the initial polymerization rates calculated between 0.1 and 0.3 of the normalized fluorescence.

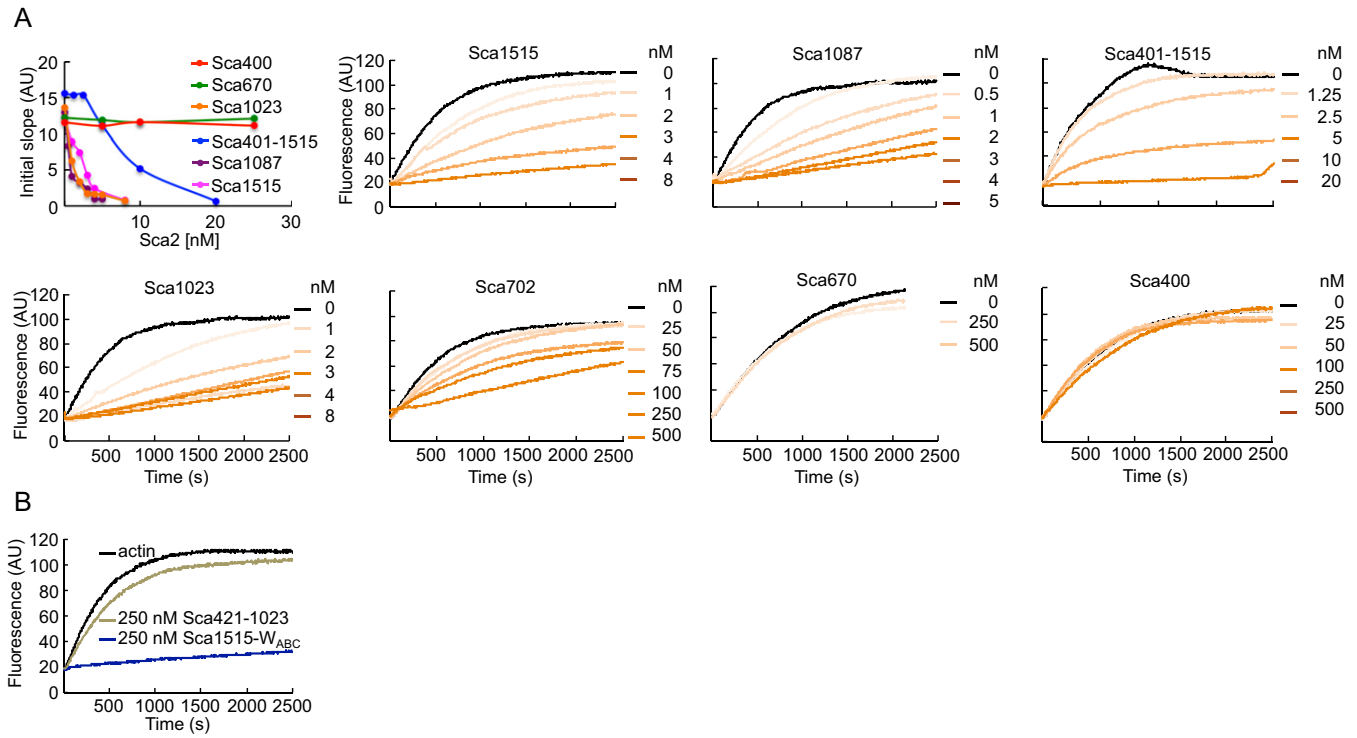

Fig. S4. Barbed-end filament elongation in the presence of Sca2 constructs. (*A*) Elongation of phalloidin-stabilized actin filament seeds (1.5 μM) in the presence of 0.5 μM actin monomers (6% pyrene-labeled) and increasing concentrations of Sca2 constructs, as indicated. The *Upper Left* figure shows a comparison of the initial slopes (arbitrary units) plotted as a function of construct concentration for some of the Sca2 constructs (color coded). (*B*) Elongation of filaments seeds in the presence of Sca1515-W_{ABC} (containing mutations in the WH2 domains; see Fig. S2*A*) and compared with Sca421-1023. The strong inhibition of elongation is consistent with barbed-end capping by Sca1515-W_{ABC}, and not monomer sequestration as observed with Sca421-1023 (Fig. S3).

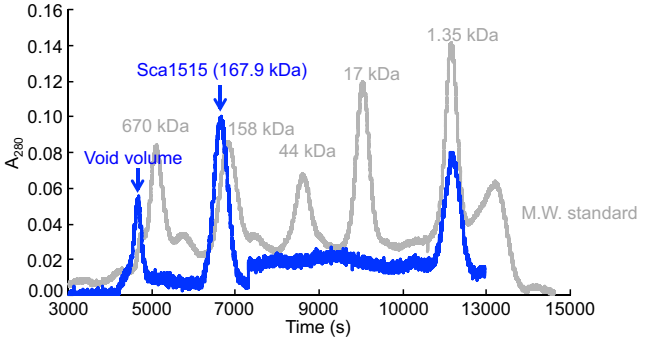

Fig. S5. Sca1515 (molecular weight 167.9 kDa) elutes as a monomer by size-exclusion chromatography. A standard sample is shown in gray for comparison.

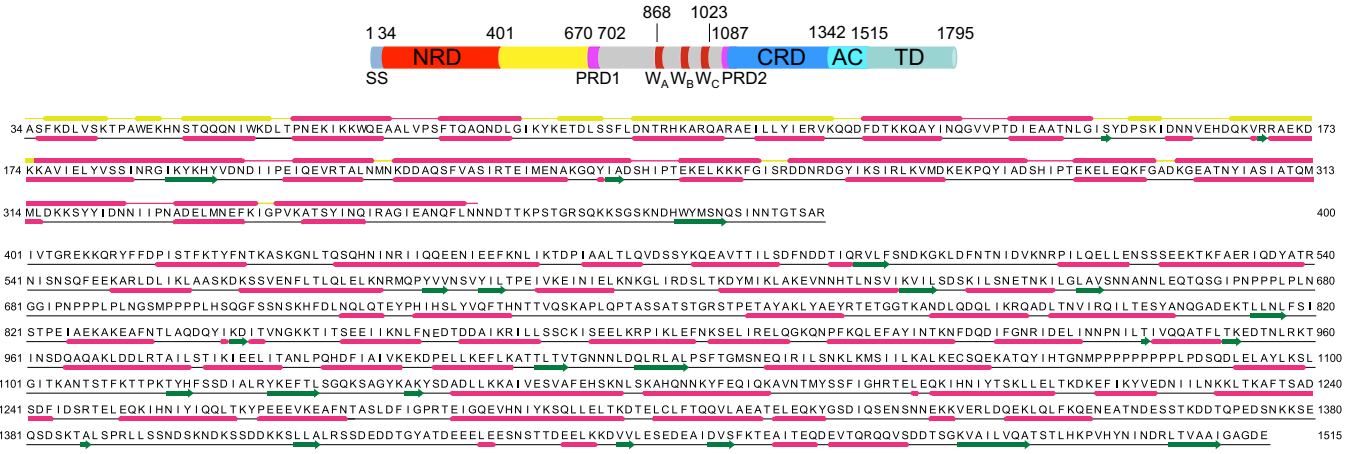

Fig. S6. The fold of the passenger domain of Sca2 is predicted to be mostly helical. Various programs consistently predict that the fold of the passenger domain of Sca2 is dominated by α-helices (red regions in the diagram) and connecting loops or less ordered regions. The secondary structure prediction shown here below the sequence is by the program Jpred3 (1). Note that although a few β-strands are predicted, most of them probably do not actually occur in the structure, as indicated by two observations: (*i*) the predicted β-strands typically occur in isolation (i.e., they do not form part of a stabilizing β-sheet or β-solenoid), and (*ii*) the crystal structure of the N-terminal repeat domain (NRD), shown separately at the top of the figure, does not contain a single β-strand, whereas a few are predicted by Jpred3 (actual secondary structure content shown above the sequence and colored according to Fig. 4*A*). Note finally that from residue 1342 onward, C-terminal to the C-terminal repeat domain (CRD), the character of the fold appears to change and is predicted to be mostly disordered with a few short α-helices and β-strands (predicted in equal amounts). In most autotransporters, this region corresponds to the so-called autochaperone domain (2), and Sca2 does not appear to be an exception to this rule. Deletion of this region in Sca2 does not appear to affect the overall actin polymerization activity (Fig. 1*E*). AC, autochaperone domain; TD, translocator domain.

1. Cole C, Barber JD, Barton GJ (2008) The Jpred 3 secondary structure prediction server. *Nucleic Acids Res* 36(Web Server issue):W197–W201.
2. Benz I, Schmidt MA (2011) Structures and functions of autotransporter proteins in microbial pathogens. *Int J Med Microbiol* 301(6):461–468.

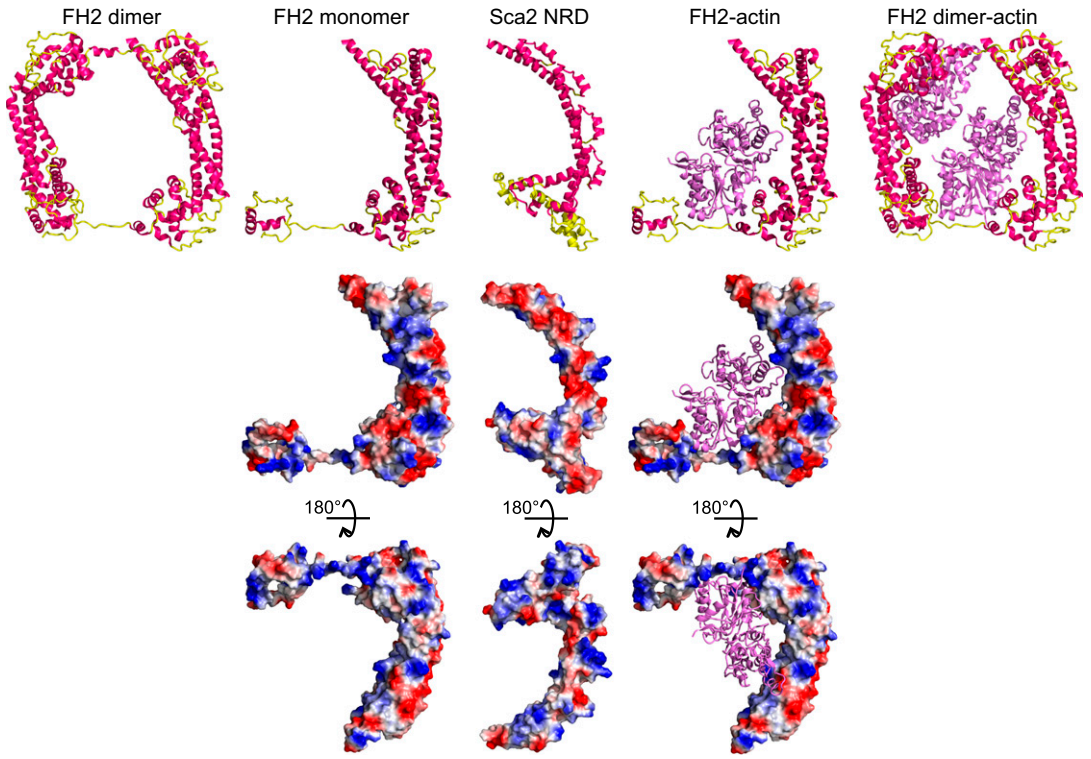

Fig. S7. The NRD of Sca2 (*Middle*) has a crescent-shaped structure that resembles that of a monomer of the formin FH2 fold (*Left* and *Right*; PDB code: 1Y64). The CRD is predicted to also share this fold (see also Fig. 4 and Fig. S6). The figure shows ribbon (*Top*) and electrostatic surface representations (*Bottom*) in which positively and negatively charged surfaces are colored blue and red, respectively. Actin is colored violet and the FH2 is colored red (helices) and yellow (loops). The NRD is colored red (repeats) and yellow (nonrepeat regions) according to Fig. 4*A*. The FH2 dimer shown here was assembled from two crystallographically independent subunits of the structure of the FH2 domain of yeast Bni1p in complex with actin (1). The similarity in shape between the two unrelated folds suggests that actin may bind in the concave side of the NRD crescent (see Fig. S8 for evidence in support of this prediction).

1. Otomo T, et al. (2005) Structural basis of actin filament nucleation and processive capping by a formin homology 2 domain. *Nature* 433(7025):488–494.

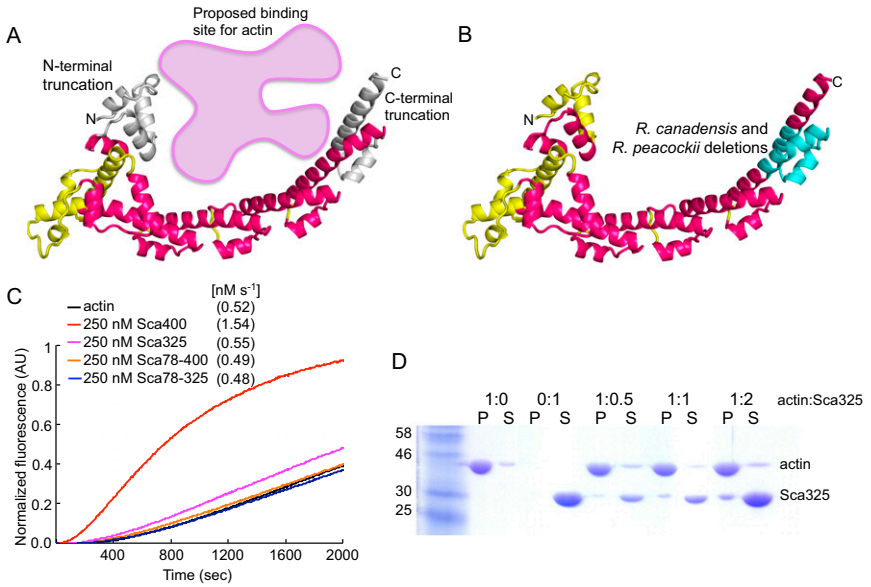

Fig. S8. Analysis of the nucleation and F-actin-binding activities of deletion mutants of NRD. (*A*) The regions of NRD deleted to produce constructs Sca78-400, Sca325, and Sca78-325 are shown in gray. A cartoon representing the predicted binding site for actin (by analogy with the FH2 fold, see Fig. S7) is also shown (magenta). (*B*) A deletion in the NRDs of *R. peacockii* and *R. canadensis* Sca2 (cyan), may explain why these species do not form actin tails (see also Fig. S1). (*C*) Normalized time course of polymerization of 2 μM Mg ATP-actin (6% pyrene-labeled) alone (black) or in the presence of 250 nM Sca2 constructs, as indicated. Initial rates are shown in parenthesis. (*D*) SDS/PAGE analysis of supernatant (S) and pellet (P) fractions after cosedimentation at 278,000*g* of F-actin (15 μM) with increasing ratios of Sca325. Controls, F-actin and Sca325 alone, are also shown.

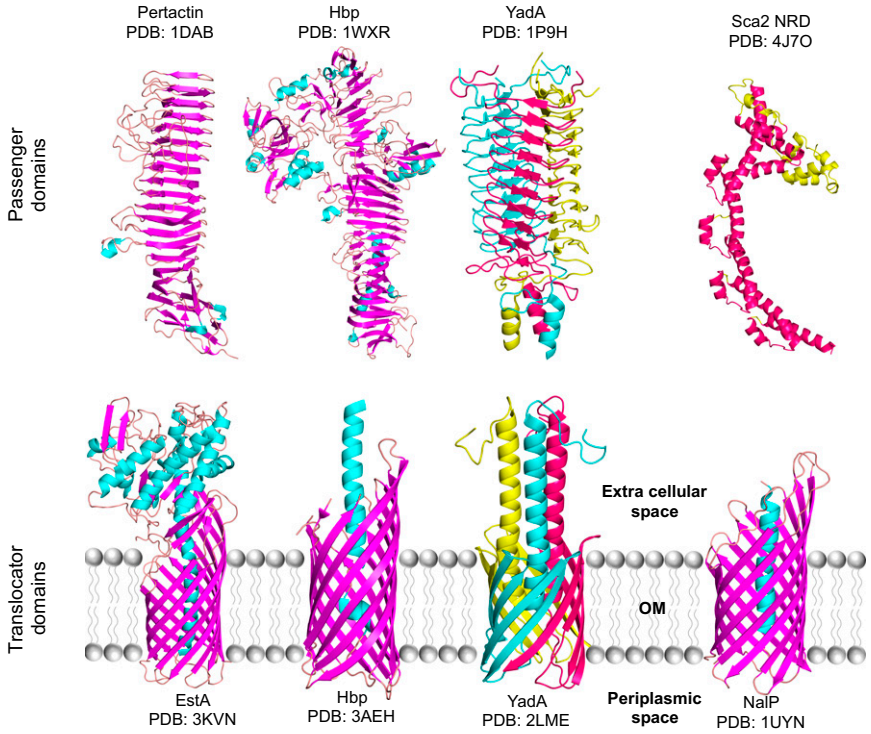

Fig. S9. Comparison of the structure of Sca2's NRD with those other autotransporters (PDB accession codes are indicated). The passenger domains of most autotransporters form β-solenoid structures, contrary to the NRD that forms an all-helical structure. The rest of Sca2 is also predicted to consist primarily of α-helices (Fig. 4 and Fig. S6). The C-terminal translocator domain of autotransporters forms a pore at the outer membrane for secretion of the large N-terminal passenger domain. Translocator domains are either ∼300- or ∼75-aa long, giving rise to two types of autotransporters, monomeric and trimeric, whereby the 12 strands of the β-barrel that forms the translocation pore are all contributed by a single chain or by three chains. With a 281-aa translocator domain, Sca2 clearly belongs to the monomeric subgroup of autotransporters. Sca2's passenger domain is also a monomeric is solution (Fig. S4).

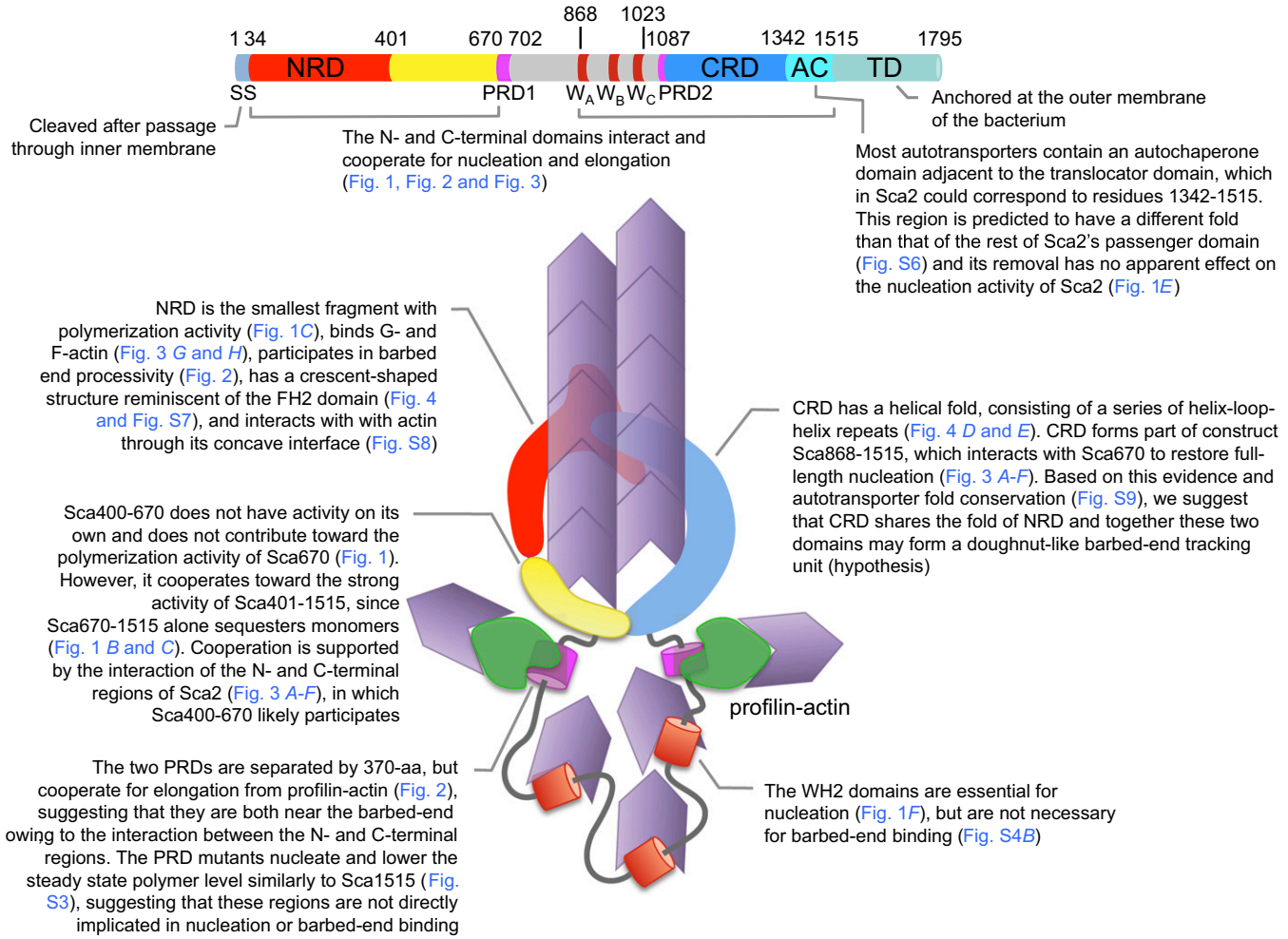

Fig. S10. Model of nucleation and elongation of Sca2 and experimental evidence provided in this article that supports this model (related to Fig. 5).

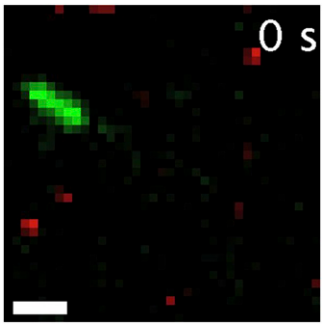

Movie S1. Visualization by total internal reflection fluorescence (TIRF) microscopy of filament assembly induced by Sca1515-quantum dot (Qdot) with 1.5 μM ATP-actin and 4 μM profilin (corresponding to Fig. 2*B*). Arrows point to Sca1515-Qdot (red) bound to the barbed end of an actin filament (green). A white asterisk indicates a filament-buckling event. (Scale bar, 1 μm; magnification, 100× 1.45 N.A. objective.)

Movie S1

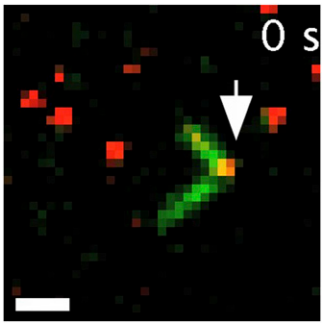

Movie S2. Visualization by TIRF microscopy of filament assembly induced by Sca401-1515-Qdot with 1.5 μM ATP-actin and 4 μM profilin (corresponding to Fig. 2*B*). Arrows point to Sca401-1515-Qdot (red) bound to the barbed end of an actin filament (green). A white asterisk indicates a filament-buckling event. (Scale bar, 1 μm; magnification 100× 1.45 N.A. objective.)

Movie S2

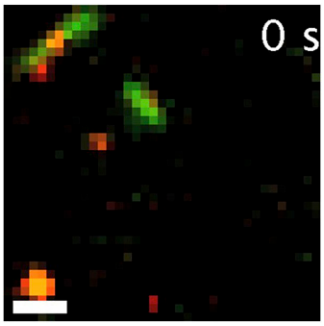

Movie S3. Visualization by TIRF microscopy of filament assembly induced by Qdot-Sca1023 with 1.5 μM ATP-actin and 4 μM profilin (corresponding to Fig. 2*B*). Arrows point to Qdot-Sca1023 (red) bound to the barbed end of an actin filament (green). A white asterisk indicates a filament-buckling event. (Scale bar, 1 μm; magnification 100× 1.45 N.A. objective.)

Movie S3

Movie S4. A 360° rotation of the structure of NRD.

Movie S4